Supplemental information

Supplemental Methods

Reagents

Papain, collagenase H, dithiothreitol (DTT), dithioerythritol (DTE), ovalbumin (OVA), aluminum hydroxide, niflumic acid (NA), nifedipine, caffeine, tetraethylammonium chloride (TEA) and isoproterenol (ISO) were purchased from Sigma (St. Louis, MO, USA). Fluo-4 AM was purchased from Invitrogen (Eugene, OR, USA). Paxilline was obtained from Cayman Chemical (Ann Arbor, MI, USA). Ryanodine, the anti-TMEM16A antibody, and the anti-BK channel β1 and β4 subunit antibodies were purchased from Alomone Labs (Jerusalem, Israel). The anti-BK channel alpha antibody was purchased from Abcam (Cambridge, MA, USA). The anti-BK-FITC antibody was purchased from Biorbyt (Berkeley, CA, USA). Niflumic acid, nifedipine, ryanodine and fluo-4 AM were dissolved in DMSO; the others were dissolved in the corresponding solutions.

Animals

Six-week male C57BL/6 mice and eight-week male Wister rats were purchased from the Hubei Provincial Centers for Disease Control and Prevention (Wuhan, China) and housed under controlled temperatures (21-23 °C) and lighting conditions (lights on 8:00-20:00) with ad libitum access to water and food. All experiments were approved by the Institutional Animal Care and Use Committee of the South-Central University for Nationalities.

Human airway and cerebral artery smooth muscle

Human airway smooth muscle (ASM) was obtained from the tracheae and/or bronchi of lung transplant donors, recipients and/or resected carcinoma tissues. Human cerebral artery smooth muscle was obtained from tissues resected from brain tumors. Written informed consents were signed, and the experiments were approved by the Ethics Committee of the South-Central University for Nationalities.

Isolation of single mouse and human ASMCs and CASMCs

Single mouse ASMCs and CASMCs were enzymatically isolated from the tracheae and cerebral arteries of BALB/c mice and Wister rats, respectively, according to the previous protocol [1-4]. In brief, animals were euthanized by intraperitoneal injection of sodium pentobarbital (150 mg/kg). The tracheae and cerebral basilar arteries were quickly removed and placed in ice-cold low Ca^{2+} physiological saline solutions (LCPSS) containing 135 mM NaCl, 5 mM KCl, 1 mM $MgSO_4$, 10 mM glucose, 10 mM HEPES, and 0.1 mM $CaCl_2$ (pH 7.4, adjusted with NaOH). The tracheae and arterial smooth muscles were isolated, minced and then incubated for 22-25 min at 35 °C in LCPSS containing 1 mg/mL papain, 0.2 mg/mL DTE, and 1 mg/mL BSA and then transferred to LCPSS containing 1 mg/mL collagenase H, 0.2 mg/mL DTT and 1 mg/mL BSA for 8-10 min. The tissue was then washed and gently triturated in LCPSS to yield single cells, which were stored on ice and used for experiments within 4 h. Single human ASMCs and CASMCs were similarly isolated.

Measurements of Ca^{2+} sparks and cell length

Cells were loaded with 2.5 μM fluo-4 AM in physiological saline solutions (PSS) containing 135 mM NaCl, 5 mM KCl, 1 mM $MgCl_2$, 2 mM $CaCl_2$, 10 mM HEPES, and 10 mM glucose (pH 7.4, adjusted with NaOH). Ca^{2+} sparks were measured using an LSM 700 laser scanning confocal microscope (Carl Zeiss, Göttingen, Germany) as previously described [5-7]. The frequency and amplitude of the Ca^{2+} sparks [5-7] were analyzed using Zen 2010 software (Carl Zeiss, Göttingen, Germany) and Origin 9.0 software (OriginLab, Northampton, MA, USA).

The measurement of cell length with [5] and without [1] Ca^{2+} sparks was performed using the LSM 700 laser scanning confocal microscope and analyzed using the Zen 2010 software. The cell length measurement in single cells will avoid the stretching-induced increases in Ca^{2+} sparks and cytosolic Ca^{2+} [8], allowing us to study the role of physiological Ca^{2+} sparks.

Measurement of cell length

Cells isolated from one mouse or one subject were placed in 1 mL PSS, which was then randomly and evenly divided and transferred into two tubes. Inhibitor(s) and vehicle were respectively added to the tubes. Both tubes were shaken slowly for 15 min at room temperature. The cells from the two tubes were respectively dropped in a chamber; 10 min later, the transmitted light images of cells were acquired using the LSM 700 confocal microscope, and the cell lengths were measured with Zen 2010 software.

Measurements of the airway lumen area

Tracheal rings (TRs) were cut from the distal end of mouse tracheae and placed in the

chamber. The airway lumen area (ALA) was measured using the LSM 700 confocal microscope. This approach will allow us to observe the relaxation of ASMCs. Because the elastic force produced by the tracheal cartilages will pull airway smooth muscle to prolongation, and then to result in ALA increases. This method was tested by the known bronchodilator isoproterenol (ISO) (Fig. S1).

Recordings of ion channel currents and membrane potential

Ion channel currents were recorded using the patch clamp technique with an EPC-10 patch-clamp amplifier (HEKA, Germany). STICs, STOCs, and caffeine-induced currents were recorded using whole-cell configurations [2, 3]. Patch pipettes had a resistance of 3 to 5 ΩM when filled with an intracellular solutions containing 139 mM KCl, 1 mM $MgCl_2$, 10 mM HEPES, and 3 mM Na_2ATP (pH 7.2, adjusted with KOH). The bath solutions were PSS. The holding potential was -45 mV. The junction potential, capacitance, and series resistance were compensated. A 30s step was applied from -60 to 10 mV in increments of 10 mV to record the STICs and STOCs. Voltage ramps from -80 to 60 mV for 320 ms or a long step at -60 mV were applied to measure the caffeine-induced whole-cell currents.

LVDCCs-mediated currents were recorded using barium (Ba^{2+}) as the charge carrier [9, 10]. The holding potential was -70 mV, and the LVDCC currents were recorded from -60 to 40 mV for 300 ms with a 10-mV increment. Leak currents were subtracted using a P/4 protocol. The extracellular solutions contained (mM) 126 NaCl, 10 TEA, 2.2 $BaCl_2$, 1 $MgCl_2$, 10 HEPES, and 5.6 glucose (pH 7.4, adjusted with NaOH). The pipette solutions contained (mM) 139 CsCl, 1 $MgCl_2$, 10 HEPES, 3 MgATP, and 0.5 Na_2ATP (pH 7.3, adjusted with

KOH).

Single BK channel currents were measured at potentials of 0, 20, 40, and 60 mV for 20 s from the holding potential of 0 mV using the inside-out patch-clamp technique with symmetrical K^+ ion concentrations in intracellular and extracellular solutions [3]. The intracellular solutions contained (mM) 140 KCl, 1 $MgCl_2$, 5 EGTA and 10 HEPES (pH 7.2, adjusted with KOH). The free Ca^{2+} ion concentration (1, 3, and 10 μM) in these solutions was set by adding the required amount of $CaCl_2$, which was calculated using WEBMAXC STANDARD (http://www.stanford.edu/~cpatton/webmaxc/webmaxcS.htm). Extracellular solutions contained (mM) 140 KCl, 1 $MgCl_2$, 5 EGTA, 4.9 $CaCl_2$ and 10 HEPES (pH 7.2, adjusted with KOH). The free Ca^{2+} ion concentration was 10 μM. Single-channel currents were acquired at a digitization rate of 4 kHz and filtered at 1 kHz. Events were detected, and the all-point amplitude histograms and single-channel open probabilities (*Po*) were obtained using Clampfit 9 software (Axon Instruments, USA). The histograms were fitted with the Gaussian distribution function. Peak values were obtained, and the net values were calculated and then used to construct current-voltage (I-V) curves, by which the single-channel conductance (i.e., pS value) was determined.

Vm was measured using the current-clamp configuration of the whole-cell patch clamp technique [11]. The bath solutions were PSS. The patch pipette solutions consisted of 130 mM KCl, 2.0 mM $MgCl_2$, 3.0 mM EGTA, 1.0 mM $CaCl_2$, 5.0 mM Na_2ATP, and 10 mM HEPES (pH 7.2).

Measurements of TMEM16A and BK channel mRNA

Total RNA was extracted from mouse ASMCs and CASMCs using TRIzol reagent (Invitrogen) and treated with DNase (Promega). One microgram of total RNA was reverse transcribed to synthesize cDNA using the ReverTra Ace Reverse Transcriptase Kit (Toyobo). Samples were analyzed by semi-quantitative RT-PCR and quantitative RT-PCR using the primers described in Table 1 and a Bio-Rad PCR system instrument and a 7500 Fast Real-Time PCR System instrument (Applied Biosystems, Foster City, CA, USA), respectively.

Amplification conditions for the semi-quantitative RT-PCR reactions were as follows: initial denaturation at 94 °C for 3 min; amplification at 94 °C for 30 s, 60 °C for 30 s, followed by 72 °C for 45 s for 30 cycles (TMEM16A, BK-α, BK-β1, BK-β2, BK-β3, and BK-β4) or 25 cycles (GAPDH) and extension at 72 °C for 7 min. The housekeeping gene Gapdh was used as the internal reference. The products were resolved by electrophoresis in 2% agarose gels using ethidium bromide for visualization. Images of PCR product bands were captured using a Gel Doc ^{TM} XR+ system (Bio-Rad).

The amplification conditions for the quantitative RT-PCR reactions were as follows: initial denaturation at 95 °C for 1 min and amplification at 95 °C for 15 s, 60 °C for 30 s, followed by 72 °C for 30 s for 40 cycles (GAPDH, TMEM16A, BK-α, BK-β1, BK-β2, BK-β3, and BK-β4). The housekeeping gene GAPDH was used as the internal reference. The sample cycle threshold (Ct) was calculated automatically using Applied Biosystems software. The relative expression levels of samples were calculated using Ct levels of target genes normalized to that of GAPDH.

Table S1. List of primer pairs used for the measurement of TMEM16A, BK subunit and

GAPDH mRNA

Gene	GenBank accession number	Primer sequence	Product length
GAPDH	NM_008084.3	Forward, 5’-AACCTGCCAAGTATGATGACAT-3’ Reverse, 5’-CCTGTTGCTGTAGCCGTATT-3’	201 bp
TMEM16A	NM_178642.5	Forward, 5’-CCGAATCTCAGGCTTCCAAGGT-3’ Reverse, 5’-ATGAACGCTCAGCCACAGTCTC-3’	255 bp
BK-α	NM_001253378.1	Forward, 5’-GGATGGTGGTTGTTATGGT-3’ Reverse, 5’-CTTACTGGACGACTGTGAG-3’	262 bp

BK-β1	NM_031169.4	Forward, 5’-GTCGCTTCTTCGTGGTAA-3’ Reverse, 5’-TCTTAGGTGACTCCTGTGA-3’,	175 bp
BK-β2	NM_028231.2	Forward, 5’-TGTGGAATGAACGGTGAA-3’ Reverse, 5’-GTTTGGATAGTCATGGGTTT-3’	186 bp
BK-β3	NM_001195074.1	Forward, 5’-CTTCTCCACTACGACGAC-3’ Reverse, 5’-CCTAACCAAGCCAACAATC-3’	270 bp
BK-β4	NM_021452.1	Forward, 5’-AACCAGAAGAACTCGGAGA-3’ Reverse, 5’-GGACCACGATGAGAACAC-3’,	202 bp

Immunofluorescence staining

TMEM16A [12, 13] and BK channel expression [14] in single mouse cells were investigated using immunofluorescence staining. Cells were fixed using 4% paraformaldehyde and permeabilized with 0.5% Triton X-100. For TMEM16A detection, cells were incubated with anti-TMEM16A antibodies at 4 °C overnight, followed by incubation with FITC-goat anti-rabbit IgG. For BK staining, cells were incubated with anti-BK-FITC antibody at 4 °C overnight. The FITC fluorescence intensity was then measured using the LSM 700 confocal microscope.

Supplemental Results

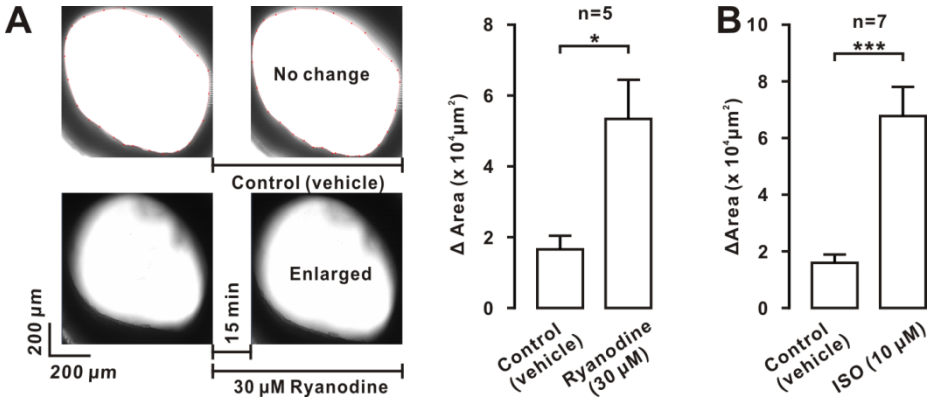

Fig. S1 Ryanodine and ISO increase the lumen area of the mouse airway. (A) The tracheal lumen area increased following incubation with 30 µM ryanodine. The area did not change in the control experiment. The summary of the results demonstrates that the ryanodine-induced increase in the area was significant compared to that in the control. **(B)** ISO induced a similar increase in the area. *: $P < 0.05$; ***: $P < 0.001$. These data indicate that ASMC relaxation resulted in ALA increases, and that the abrogation of Ca^{2+} sparks by

ryanodine elongated the ASMCs, suggesting that Ca^{2+} sparks increased ASMC tone.

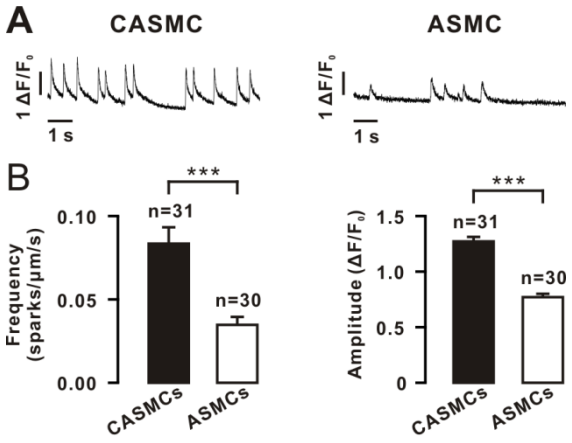

Fig. S2 Differences in Ca^{2+} sparks in mouse CASMCs and ASMCs. (A) Ca^{2+} sparks were measured in both cell types. **(B)** Their average frequency and amplitude were calculated and both were higher in CASMCs than in ASMCs. ***: $P < 0.001$. These results indicate that Ca^{2+} sparks were more and had higher amplitude in CASMCs compared to ASMCs.

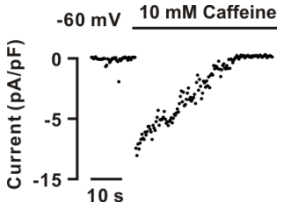

Fig. S3 Rat CASMCs have functional Clca channels. Caffeine induced large inward currents in 6 cells, suggesting these cells would have functional Clca channels.

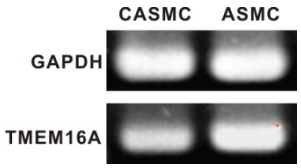

Fig. S4 TMEM16A mRNA is detected in mouse CASMCs and ASMCs. TMEM16A mRNA was measured by RT-PCR, showing that it was abundant in both cells; however, the

level was lower in CASMCs than in ASMCs. GAPDH mRNA was the internal reference. Three independent experiments were performed, and similar results were observed.

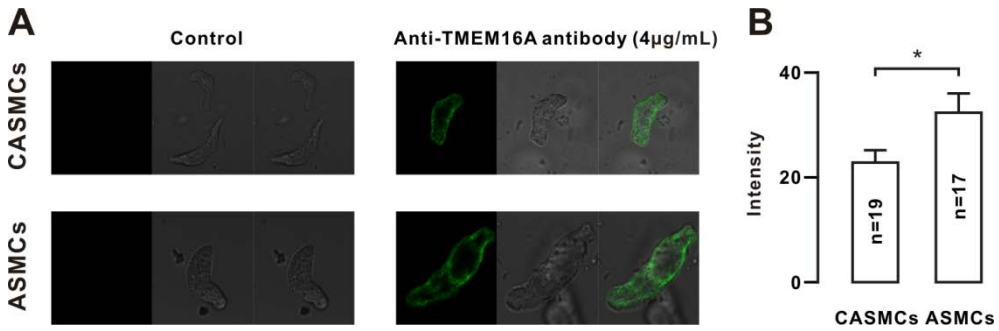

Fig. S5 TMEM16A protein is detected in mouse CASMCs and ASMCs. (A) Both types of cells were permeabilized, incubated with or without anti-TMEM16A antibodies, and then incubated with FITC-goat anti-rabbit IgG. The images of FITC staining and transmitted light were acquired and then overlapped. **(B)** The intensity of the FITC fluorescence was summarized, indicating both cell types expressed TMEM16A; however, the FITC intensity was lower in CASMCs than in ASMCs. *: $P < 0.05$.

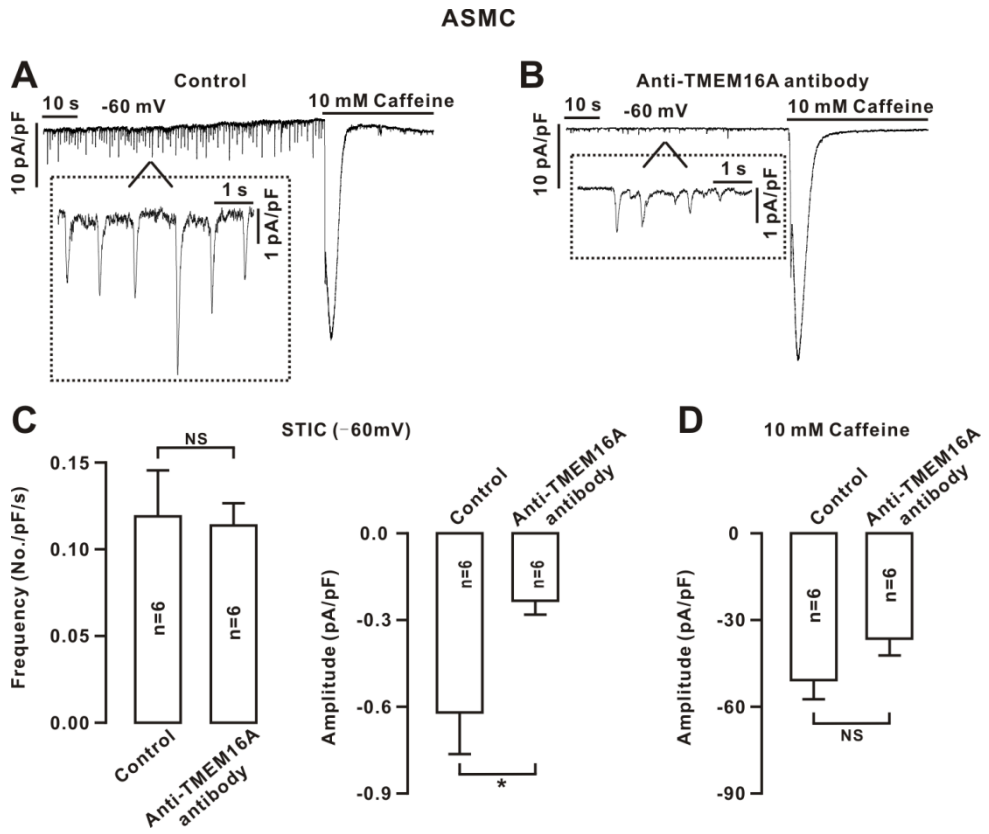

Fig. S6 Effects of anti-TMEM16A antibodies on Ca^{2+}-activated inward currents in mouse ASMCs. (A) STICs and caffeine-induced inward currents were recorded in an ASMC. STICs are shown in the i*nset* box. **(B)** The same recordings in an ASMC incubated with anti-TMEM16A antibodies. **(C)** The average frequency and amplitude of STICs were summarized, indicating that the antibodies induced a decrease in the amplitude but did not affect the frequency. **(D)** The average amplitude of the caffeine-induced currents, showing that the antibodies failed to significantly alter the currents. NS: $P > 0.05$; *: $P < 0.05$. These data indicate that TMEM16A failed to affect the frequency of STICs, however, increased the amplitude of STICs, but did not significantly affect the amplitude of caffeine-induced inward currents.

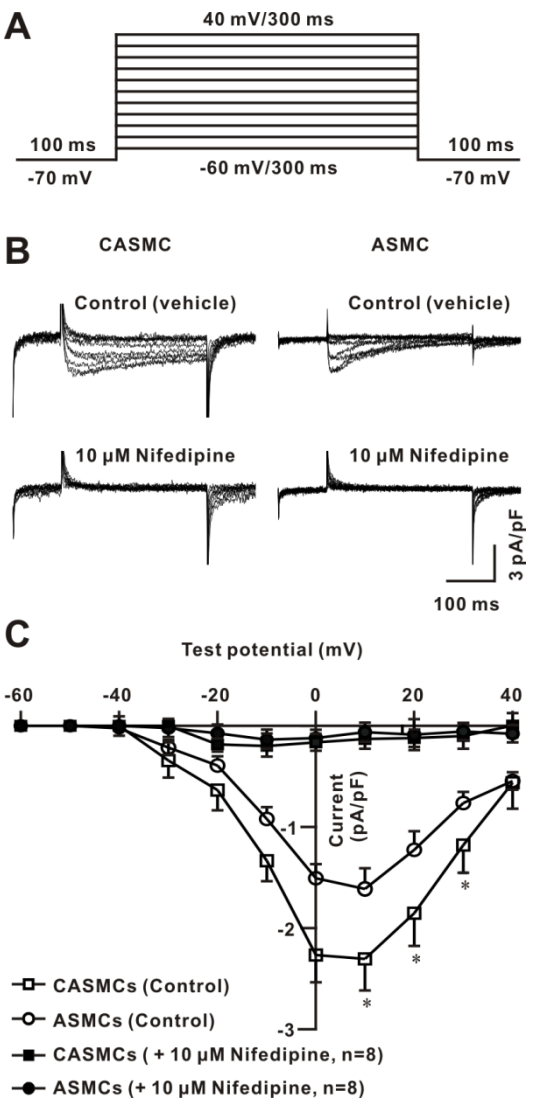

Fig. S7 LVDCCs-mediated currents in mouse CASMCs and ASMCs. (A) The protocol used to record LVDCC-mediated currents. **(B)** The currents were blocked by nifedipine, a selective blocker of LVDCCs. **(C)** Current-voltage (I-V) curves. *: $P < 0.05$. These data demonstrate that LVDCCs were expressed in both cell types and were activated around -40 mV; however, LVDCC-mediated currents were larger in CASMCs than in ASMCs.

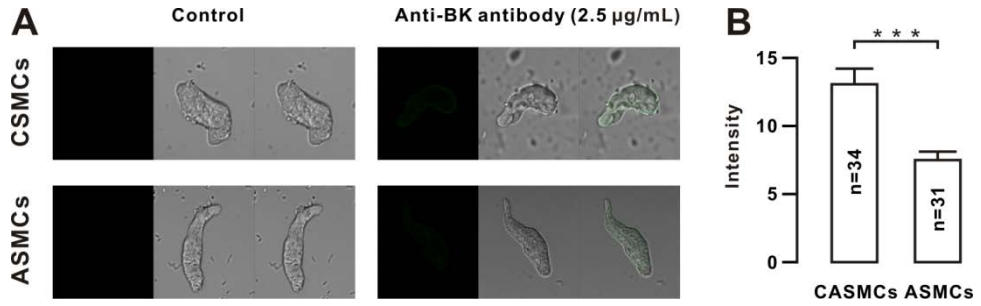

Fig. S8 BK staining in mouse cells. (A) CASMCs and ASMCs were permeabilized and incubated with and without anti-BK-FITC antibodies. The images of the FITC fluorescence and transmitted light were acquired and overlapped. **(B)** The FITC intensity was summarized, showing that TMEM16A levels were lower in CASMCs than in ASMCs. ***: P < 0.001.

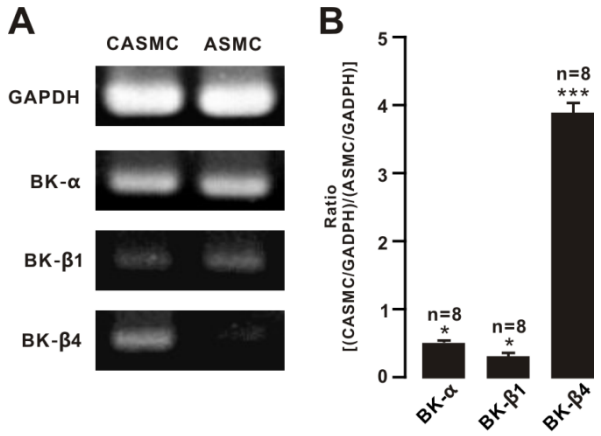

Fig. S9 mRNA levels of BK subunits in mouse CASMCs and ASMCs. (A) mRNA expression of BK subunits was measured using semi-quantitative RT-PCR. α, β1 and β4 mRNA were detected, and α and β1 levels were lower and β4 levels were higher in CASMCs than in ASMCs. These results were observed in 8 separate experiments. GAPDH was used as the internal reference. **(B)** The mRNA levels of these three subunits were further quantified using quantitative RT-PCR, and the ratios between the two cell types were calculated and compared. *: P < 0.05; ***: P < 0.001.

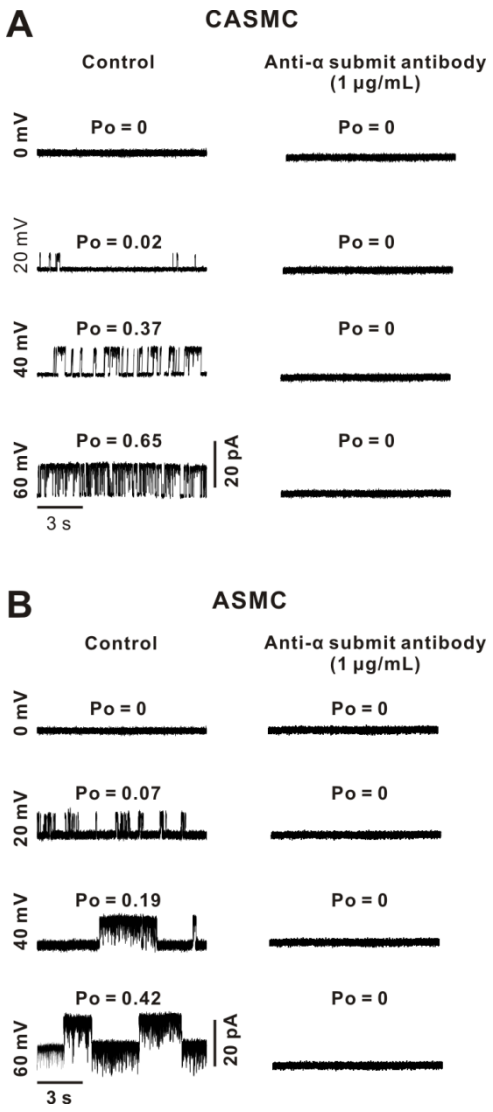

Fig. S10 Single BK currents are abolished by anti-α subunit antibodies. (A) Single BK channel-mediated currents were recorded in a patch of membrane from a mouse CASMC at 0, 20, 40 and 60 mV under 1 μM Ca^{2+} and were blocked by 1 μg/mL anti-α subunit antibodies. These results were observed in 4 patches. **(B)** The same experiments were performed in 4 patches from ASMCs. These results indicate that α subunits were the pore-forming subunits for BKs.

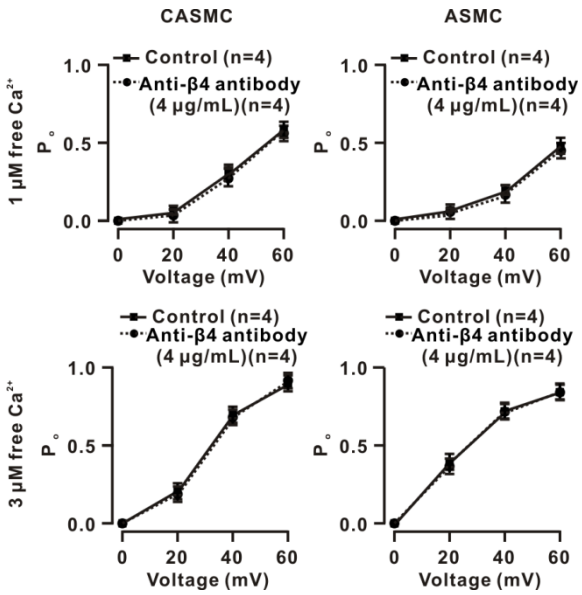

Fig. S11 Effects of anti-β4 subunit antibodies on single BK currents in mouse cells. Single BK currents were similarly recorded and analyzed. The results show that the *Po* values were not affected by anti-β4 subunit antibodies in patches from CASMCs and ASMCs.

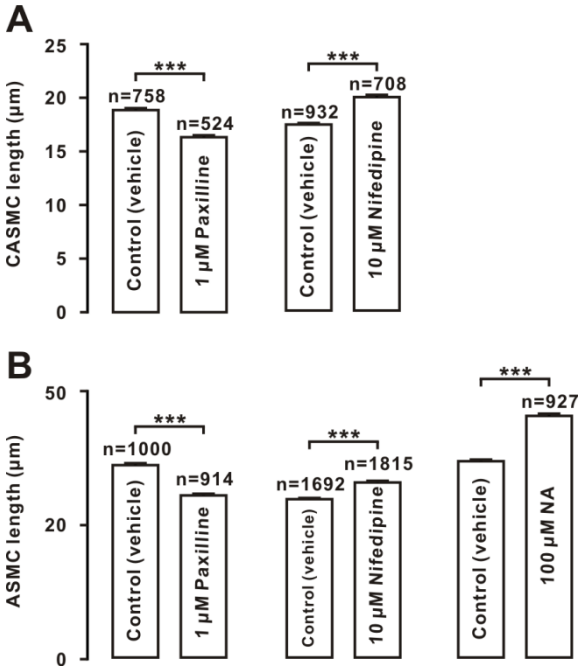

Fig. S12 Effects of NA, paxilline and nifedipine on cell length. (A) Mouse CASMCs were shortened by paxilline and elongated by nifedipine. **(B)** Mouse ASMCs were elongated by NA and nifedipine and shortened by paxilline. ***: $P < 0.001$. These results showed the

effects of Clca channels, LVDCCs and BKs on tone in two cell types.

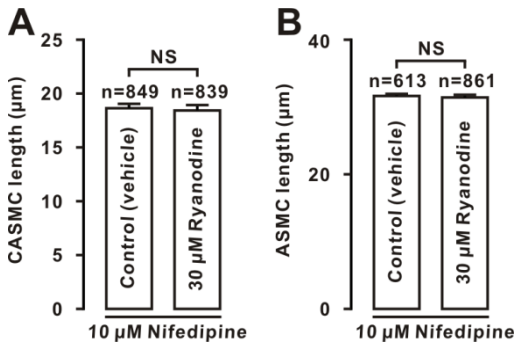

Fig. S13 Nifedipine blocks ryanodine-induced changes in cell length. (A) Mouse CASMCs and **(B)** ASMCs were incubated with nifedipine for 15 min and then with vehicle and ryanodine for 15 min. The cell length was measured. NS: $P > 0.05$. The results show that the ryanodine-induced shortening of CASMCs and elongating of ASMCs were blocked by nifedipine, indicating that LVDCCs will be the final mediator for the effects of Ca^{2+} sparks on tone in both cell types.

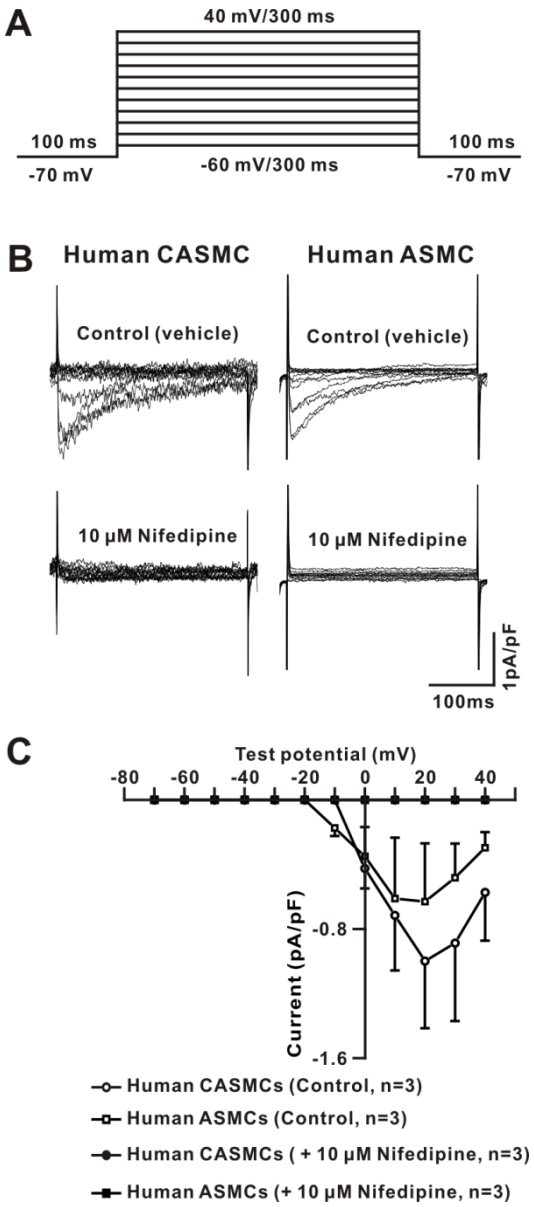

Fig. S14 Both types of human cells have LVDCCs. (A) The protocol used to record LVDCCs-mediated currents. **(B)** The LVDCC currents in a human CASMC and ASMC were recorded and then blocked by nifedipine. **(C)** I-V curves were plotted. These results indicate that both types of human cells had LVDCCs.

References

1. Liu QH, Zheng YM, Korde AS, Yadav VR, Rathore R, Wess J, et al. Membrane depolarization causes a direct activation of G protein-coupled receptors leading to local Ca2+ release in smooth muscle. Proc Natl Acad Sci U S A. 2009; 106: 11418-23.

2. Zhang T, Luo XJ, Sai WB, Yu MF, Li WE, Ma YF, et al. Non-selective cation channels mediate chloroquine-induced relaxation in precontracted mouse airway smooth muscle. PLoS One. 2014; 9:

e101578.
3. Wei MY, Xue L, Tan L, Sai WB, Liu XC, Jiang QJ, et al. Involvement of large-conductance Ca2+-activated K+ channels in chloroquine-induced force alterations in pre-contracted airway smooth muscle. PLoS One. 2015; 10: e0121566.
4. Dong L, Zheng YM, Van Riper D, Rathore R, Liu QH, Singer HA, et al. Functional and molecular evidence for impairment of calcium-activated potassium channels in type-1 diabetic cerebral artery smooth muscle cells. J Cereb Blood Flow Metab. 2008; 28: 377-86.
5. Tuo QR, Ma YF, Chen W, Luo XJ, Shen J, Guo D, et al. Reactive oxygen species induce a Ca(2+)-spark increase in sensitized murine airway smooth muscle cells. Biochem Biophys Res Commun. 2013; 434: 498-502.
6. Liu QH, Zheng YM, Wang YX. Two distinct signaling pathways for regulation of spontaneous local Ca2+ release by phospholipase C in airway smooth muscle cells. Pflugers Arch. 2007; 453: 531-41.
7. Liu QH, Zheng YM, Korde AS, Li XQ, Ma J, Takeshima H, et al. Protein kinase C-epsilon regulates local calcium signaling in airway smooth muscle cells. Am J Respir Cell Mol Biol. 2009; 40: 663-71.
8. Ji G, Barsotti RJ, Feldman ME, Kotlikoff MI. Stretch-induced calcium release in smooth muscle. J Gen Physiol. 2002; 119: 533-44.
9. Sai WB, Yu MF, Wei MY, Lu Z, Zheng YM, Wang YX, et al. Bitter tastants induce relaxation of rat thoracic aorta precontracted with high K(+). Clin Exp Pharmacol Physiol. 2014; 41: 301-8.
10. Zhang CH, Lifshitz LM, Uy KF, Ikebe M, Fogarty KE, ZhuGe R. The cellular and molecular basis of bitter tastant-induced bronchodilation. PLoS Biol. 2013; 11: e1001501.
11. Xiao JH, Zheng YM, Liao B, Wang YX. Functional role of canonical transient receptor potential 1 and canonical transient receptor potential 3 in normal and asthmatic airway smooth muscle cells. Am J Respir Cell Mol Biol. 2010; 43: 17-25.
12. Thomas-Gatewood C, Neeb ZP, Bulley S, Adebiyi A, Bannister JP, Leo MD, et al. TMEM16A channels generate Ca(2)(+)-activated Cl(-) currents in cerebral artery smooth muscle cells. Am J Physiol Heart Circ Physiol. 2011; 301: H1819-27.
13. Caci E, Scudieri P, Di Carlo E, Morelli P, Bruno S, De Fino I, et al. Upregulation of TMEM16A Protein in Bronchial Epithelial Cells by Bacterial Pyocyanin. PLoS One. 2015; 10: e0131775.
14. Bukiya A, Dopico AM, Leffler CW, Fedinec A. Dietary cholesterol protects against alcohol-induced cerebral artery constriction. Alcohol Clin Exp Res. 2014; 38: 1216-26.